

Experimental realization of highly-efficient broadband coupling of single quantum dots to a photonic crystal waveguide

T. Lund-Hansen^{1,*}, S. Stobbe¹, B. Julsgaard^{1,†}, H. Thyrrestrup¹, T. Sünner², M. Kamp², A. Forchel², and P. Lodahl^{1‡}

¹*DTU Fotonik, Department of Photonics Engineering,*

Technical University of Denmark, Ørstedts Plads 343, DK-2800 Kgs. Lyngby, Denmark

²*Technische Physik, Universität Würzburg, Am Hubland, D-97074 Würzburg, Germany*

(Dated: November 2, 2018)

We present time-resolved spontaneous emission measurements of single quantum dots embedded in photonic crystal waveguides. Quantum dots that couple to a photonic crystal waveguide are found to decay up to 27 times faster than uncoupled quantum dots. From these measurements β -factors of up to 0.89 are derived, and an unprecedented large bandwidth of 20 nm is demonstrated. This shows the promising potential of photonic crystal waveguides for efficient single-photon sources. The scaled frequency range over which the enhancement is observed is in excellent agreement with recent theoretical proposals taking into account that the light-matter coupling is strongly enhanced due to the significant slow-down of light in the photonic crystal waveguides.

PACS numbers: 78.47.-p, 42.50.Ct, 78.67.Hc

The ability to control light-matter dynamics using photonic crystals has been demonstrated experimentally within the last few years [1, 2, 3, 4, 5]. A particularly attractive application of photonic crystals is on-chip single-photon sources. A highly efficient single-photon source is the key component required in many quantum communication protocols [6] and will allow implementing linear optics quantum computing [7]. Single photons are harvested when a quantum dot (QD) is coupled efficiently to an enhanced optical mode. One very successful approach has been to couple single QDs to a photonic crystal nanocavity [1, 2, 3]. In this process, photons are emitted with large probability to the *localized mode* of the cavity at a strongly enhanced rate. One drawback of this approach, however, is that the photons subsequently must be coupled out of the cavity, which will reduce the overall efficiency of the device significantly. Furthermore, nanocavity single-photon sources only operate within a narrow bandwidth determined by the high Q factor of the cavity. Very recently it was proposed that photonic crystal waveguides (PCWs) provide a way of overcoming these limitations [8, 9, 10, 11], which was inspired by early work of Kleppner on metallic waveguides [12]. Here we present the experimental verification that single QDs can be coupled efficiently to the mode of a PCW.

PCWs offer the possibility to tailor the dispersion of light by proper design of the structure. In this way impressive light slow-down factors of 300 have been experimentally demonstrated [13]. The efficient slow-down of the PCW mode implies that the light-matter coupling strength will be largely enhanced. This enhanced coupling will allow the efficient channeling of single photons from a QD into the PCW mode. In this case, the photons are transferred directly to the *propagating mode* of the PCW, which is fundamentally different from the cavity case, and implies that the overall efficiency of the source is potentially very high. Furthermore, the enhancement

in a PCW is not limited to a narrow spectral bandwidth as in a cavity, and precise control over the QD position is not required. Consequently demands for spatial and spectral tuning of the emitter are less stringent for PCWs than for photonic crystal nanocavities [3].

In this Letter, we present time-resolved spontaneous emission measurements on single QDs positioned in PCWs. The PCWs are formed by leaving out a single row of holes in the triangular lattice of the photonic crystal, see inset of Fig. 1. The photonic crystals are fabricated using electron beam lithography followed by dry and wet etching. In this way 150 nm thick GaAs membranes are obtained containing a single layer of self-assembled InAs QDs at the center. The density of QDs is $\sim 250 \mu\text{m}^{-2}$ with a ground state emission wavelength centered at 960 nm and inhomogeneously broadened with a width of 50 nm. Two PCW samples have been fabricated, one with lattice parameter $a = 248 \pm 2$ nm and radius $r = (0.292 \pm 0.006)a$ and one with $a = 256 \pm 2$ nm and $r = (0.286 \pm 0.006)a$. The samples are 17 μm wide and 100 μm long such that finite size effects can be neglected.

The experimental setup is shown in Fig. 1. The QDs are optically excited with a pulsed Ti:Sapphire laser operating at 800 nm with a pulse length of ~ 2 ps and a repetition rate of 75 MHz. Excitation is done through a high numerical aperture microscope objective ($NA = 0.8$) in order to limit the contribution from QDs outside the PCW. The fraction of the spontaneously emitted photons that couple to radiation modes are collected through the same microscope objective and subsequently focussed to a single mode fiber that acts as a confocal pinhole for spatial selection. The spatial resolution is found to be 1.4 μm (cf. diameter of collection area indicated in Fig. 1) by determining the distance over which the sample can be moved relative to the collection optics before the emission from a single QD is halved. The spatially

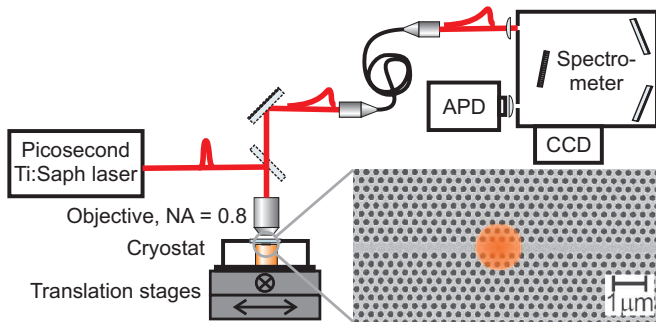


Figure 1: (Color online) Sketch of the experimental setup, which is described in detail in the text. The inset to the bottom right is a scanning electron micrograph of a fabricated PCW. The red sketched region illustrates the size of the area from which spontaneous emission is collected.

filtered spontaneous emission is coupled to a spectrometer equipped with a CCD for recording spectra (spectral resolution 0.15 nm) or an avalanche photo diode (APD) for time-correlated single-photon spectroscopy measurements (temporal resolution 280 ps). The sample is placed in a helium flow cryostat operating at 10 K. The cryostat is mounted on high-precision motorized translation stages, which enables positioning of the sample with a precision of 100 nm.

Examples of spontaneous emission spectra recorded at two different positions on a PCW ($a = 256$ nm) are displayed in Fig. 2. We observe discrete single QD emission lines. The measurements are carried out in the low excitation regime below the saturation level of single exciton lines, where predominantly spontaneous emission from the QD ground state is observed. The varying heights of the emission peaks reflect that the QD emission is redistributed depending on its position in the photonic crystal membrane [14]. In general we observe low emission from QDs that couple to the PCW. Clear spectral signatures of QD emission coupled to a PCW performed in a transmission geometry are reported in [15]. Here we employ time-resolved spontaneous emission measurements as a way to directly determine the coupling rate of photons from the QD to the PCW.

Time-resolved spontaneous emission has been recorded on single QD lines at a large number of different emission wavelengths. Two examples of decay curves that reveal very different QD dynamics are displayed in Fig. 2 (b). One of the decay curves displays a very slow single exponential decay with a rate of 0.05 ns^{-1} . This decay curve corresponds to a QD that is not coupled to the PCW, which can be due to spatial mismatch relative to the PCW or that the QD dipole moment is oriented along the PCW axis [11]. The decay rate of the uncoupled QD is inhibited by a factor ~ 20 compared to a QD in a homogeneous medium, which is an effect of the 2D photonic bandgap of the photonic crystal membrane [14, 16].

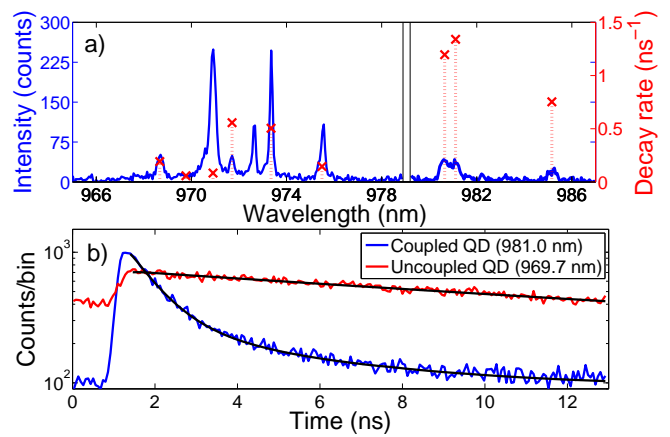


Figure 2: (Color online) (a) Spontaneous emission spectra (solid blue curve) displaying single QD emission lines. The spectra were recorded at two different positions on a PCW with $a = 256$ nm. The excitation density was $\sim 3 \text{ W/cm}^2$. The crosses indicate the measured decay rates (right axis) of the different QD emission lines. (b) Decay curves from two single QD lines. The blue decay curve is measured at 981.0 nm where the QD is coupled to the PCW. The red decay curve is measured at 969.7 nm and is an example of an uncoupled QD. The black lines are the fitted single (red curve) or double (blue curve) exponential decay models.

The decay from the other QD in Fig. 2 (b) is much faster due to coupling to the PCW mode. The fast decay curve is well described by a double exponential model, where the fast component is the rate due to coupling to the PCW, while the slow component contains contributions from dark exciton recombination in the QD [17, 18]. Note that a weak slow component also will contribute to the decay curve of the uncoupled QD, however in this case it cannot be distinguished from the inhibited decay, and a single-exponential model is sufficient. For the fast decay curve displayed in Fig. 2 (b) we derived a fast decay rate of the coupled QD of 1.34 ns^{-1} . Consequently the coupled QD decays a factor of 27 times faster than the uncoupled QD, which demonstrates that photons can be channelled very efficiently into the PCW, in agreement with recent theoretical proposals [9, 10, 11].

The complete set of in total 26 measured decay rates on the sample with $a = 256$ nm is shown in Fig. 3 (a). Here the measured decay rates are plotted as a function of scaled frequency a/λ , where λ is the emission wavelength. In modeling the data, in most cases single-exponential decay curves suffices, while only for the fastest decay curves a bi-exponential model was needed. The single-exponential model was abandoned when the properly normalized sum of the residuals characterizing the fit, i.e. the reduced χ^2 , was above 1.3. We observe a range of decay rates since differently positioned and oriented QDs couple differently to the PCW, as discussed above. Fast decay rates are only observed for a limited range of a/λ , which is in very good agreement with expectations from

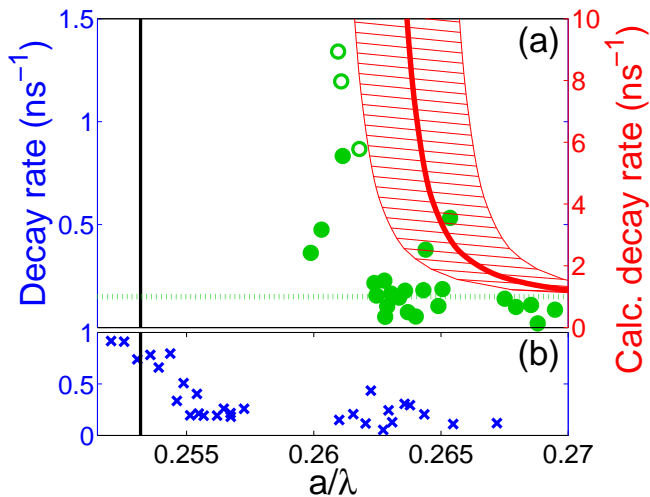


Figure 3: (Color online) (a) Measured QD decay rates on the PCW sample with $a = 256$ nm as a function of scaled frequency. The excitation power for these measurements was 3 W/cm 2 . The data points marked by open (filled) circles are modeled using a double (single) exponential decay model. The red line (right axis) displays the decay rates calculated from numerical simulations with uncertainties in a of ± 2 nm given by the hatched area. The black line at $a/\lambda = 0.253$ is the calculated band edge of the 2D photonic bandgap. The dotted green line is the mean decay rate of uncoupled QDs used for the estimation of the β -factor. (b) Measured decay rates on a photonic crystal sample with no PCW ($a = 256$ nm).

theory. Hence the most efficient coupling to the PCW occurs when the QD can couple to a slowly propagating mode, i.e. when the emission wavelength is tuned to the edge of the PCW dispersion relation.

To compare the frequency dependence of the measured decay rates with theory we have calculated the decay rate of a QD positioned in the center of the PCW using the theory of [9]:

$$\Gamma = \Gamma_0 \frac{3\pi c^3 a}{V_{\text{eff}} \omega^2 \varepsilon^{3/2} v_g(\omega)}, \quad (1)$$

where ω is the frequency of the emitter, c is the speed of light in vacuum, and ε is the electric permittivity. The group velocity (v_g) and effective mode volume (V_{eff}) have been extracted from a band structure calculation using the MPB software package [19]. Γ_0 is the decay rate in a homogeneous material, which is 1.1 ns $^{-1}$ for the QDs in this experiment. In Fig. 3 (a) we have plotted the resulting calculated decay rates (red line) assuming no adjustable parameters. A discrepancy of only 1 % is found between the frequency of enhanced decay rates in the measurement and the point of divergence of the calculated decay rate. The main uncertainty in the calculated decay rate originating from the uncertainty in a is illustrated in Fig. 3 (a) by the hatched area. Anticipating the additional uncertainty in r and ε , and the numeri-

cal uncertainty of the calculation, we conclude that there is an excellent match regarding the range of scaled frequencies where enhanced rates are observed. This clearly proves that the enhancement is due to coupling to the PCW. Our measured decay rates are found to be approximately 8 times smaller than the calculated decay rates. A lower decay rate is expected as the theory assumes a dipole emitter positioned and oriented optimally with respect to the PCW and does not take into account imperfections giving rise to scattering losses. These are known to limit the achievable group velocity slow-down factor thereby removing the divergence of the decay rate [20]. Note that scattering loss is mainly a limitation for devices relying on long propagation distances, while a single-photon source can be made very compact, thus making the use of slow-light in a photonic crystal waveguide a viable approach.

Shown in Fig. 3 (b) are the measured QD decay rates in a photonic crystal membrane ($a = 256$ nm) without a PCW. This is done in order to locate the edge of the 2D photonic bandgap of the photonic crystal in order to ensure that the enhancement discussed above is not an effect of the band edge. We observe an increase in the decay rate due to the band edge at $a/\lambda = 0.254$, which distinctly differs from the scaled frequency where the PCW coupling is observed. Furthermore, the position of the band edge matches the value found from the band structure calculation of 0.253 very well (marked by the black line in Fig. 3). Across the band edge the QD decay rates are observed to increase to around 1 ns $^{-1}$ while inside the 2D band gap decay rates between 0.05 ns $^{-1}$ and 0.43 ns $^{-1}$ are observed. The observed fluctuations reflect the dependence of the projected local density of optical states on the QD orientation and position. The measurements can be compared to the calculations of Koenderink *et al.* [16], where inhibition factors between 0.03 and 0.39 are predicted in the respective energy range of the 2D band gap.

We have collected further experimental evidence for our conclusions by investigating another PCW on a sample with lattice parameter $a = 248$ nm. In this case the slow light regime, where efficient coupling to the PCW occurs, matches the excited state of the QDs. Consequently these measurements were performed in the highly saturated regime where spontaneous emission from the QD excited states is observed. The data are presented in Fig. 4. Once again the data fall into two groups, in this case below and above ~ 0.5 ns $^{-1}$, of slow and fast rates corresponding to uncoupled and coupled QDs, respectively. The rates of the uncoupled QDs are relatively fast, since the excited states are known to have increased non-radiative decay compared to the ground state excitons. Strong enhancement is observed in this case for $a/\lambda = 0.263$, which matches theory very well. We observe enhanced rates of up to 3.5 ns $^{-1}$ clearly demonstrating the very pronounced effect of the PCW.

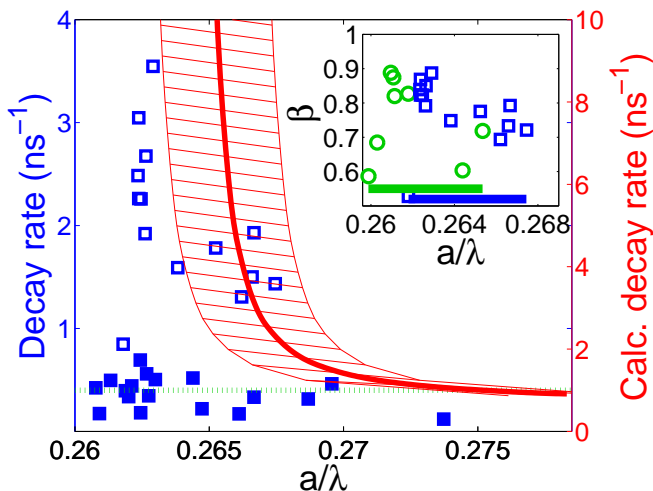


Figure 4: (Color online) Measured decay rates for QDs in a PCW sample with $a = 248$ nm. The pump excitation power was 1.5 kW/cm². The data points marked by open (filled) squares are modelled using a double (single) exponential decay model. The red line (right axis) shows the decay rates calculated from numerical simulations with uncertainties in a of ± 2 nm given by the hatched area. The dotted green line is the mean decay rate of uncoupled QDs used for the estimation of β . The inset displays the β -factors above 0.5 calculated from the data in Fig. 3 (green circles) and Fig. 4 (blue squares) as described in the text. The green (blue) bar shows the coupling bandwidth of the PCW sample with $a = 256$ nm ($a = 248$ nm).

The figure of merit determining the coupling efficiency into the PCW is the β -factor. It is defined as [9]

$$\beta = \frac{\Gamma_{\text{wg}}}{\Gamma_{\text{wg}} + \Gamma_{\text{rad}} + \Gamma_{\text{nr}}}, \quad (2)$$

where Γ_{wg} is the decay rate of the QD to the PCW, Γ_{rad} is the radiative decay rate to non-guided modes, and Γ_{nr} is the intrinsic QD non-radiative decay rate [18]. $\Gamma_{\text{tot}} \equiv \Gamma_{\text{rad}} + \Gamma_{\text{nr}}$ can be extracted from the measurements on QDs that do not couple to the PCW. The decay rate to non-guided modes will depend on position and orientation of the individual QD [11, 16], which is reflected in the variations in the decay rates of the uncoupled QDs in Fig. 3 and 4. To accommodate this we extract the average total decay rate of the uncoupled QDs, which is $\Gamma_{\text{tot}}(a = 248 \text{ nm}) = 0.4 \text{ ns}^{-1}$ and $\Gamma_{\text{tot}}(a = 256 \text{ nm}) = 0.15 \text{ ns}^{-1}$ for the two data set, respectively (marked by the green dotted line in Fig. 3 and Fig. 4). In the inset of Fig. 4 the β -factor is plotted versus scaled frequency. We observe β -factors of up to 0.89, demonstrating the excellent photon collection efficiency of PCWs. Even more spectacularly, a β -factor above 0.5 is observed in a relative bandwidth as large as 2 % (corresponding to 20 nm) for both PCW samples. This superior bandwidth is unique for a PCW. For comparison

a β -factor of 0.92 limited to a relative bandwidth of 0.3 % has been demonstrated in photonic crystal cavities [21]. This demonstrates the important advantage of PCWs for high-efficiency large bandwidth single-photon sources.

We have experimentally demonstrated that spontaneous emission from single QDs can be coupled very efficiently to a PCW. The light-matter coupling is enhanced by the light slow-down mediated by the dispersion control provided by the PCW. A β -factor as high as 0.89 and an unprecedented large bandwidth of 20 nm has been obtained, in this respect outperforming the traditional QD single-photon source approach based on narrow bandwidth cavities.

We thank Jørn M. Hvam for fruitful discussion. We gratefully acknowledge the Danish Research Agency for financial support (projects FNU 272-05-0083, 272-06-0138 and FTP 274-07-0459). BJ is supported by The Carlsberg Foundation.

* Electronic address: tolh@fotonik.dtu.dk

† Now at Physics Department, University of Aarhus, Denmark.

‡ Electronic address: pelo@fotonik.dtu.dk; URL: <http://www.fotonik.dtu.dk/quantumphotonics>

- [1] A. Kress *et al.*, Phys. Rev. B **71**, 241304(R) (2005).
- [2] D. Englund *et al.*, Phys. Rev. Lett. **95**, 013904 (2005).
- [3] K. Hennessy *et al.*, Nature **445**, 896 (2007).
- [4] S. Noda, M. Fujita, and T. Asano, Nature Photonics **1**, 449 (2007).
- [5] P. Lodahl *et al.*, Nature **430**, 654 (2004).
- [6] B. Lounis and M. Orrit, Rep. Prog. Phys. **68**, 1129 (2005).
- [7] E. Knill, R. Laflamme, and G. J. Milburn, Nature **409**, 46 (2001).
- [8] S. Hughes, Opt. Lett. B **29**, 2659 (2004).
- [9] V. S. C. Manga Rao and S. Hughes, Phys. Rev. B **75**, 205437 (2007).
- [10] V. S. C. Manga Rao and S. Hughes, Phys. Rev. Lett. **99**, 193901 (2007).
- [11] G. Lecamp, P. Lalanne, and J. P. Hugonin, Phys. Rev. Lett. **99**, 023902 (2007).
- [12] D. Kleppner, Phys. Rev. Lett. **47**, 233 (1981).
- [13] Y. Vlasov, M. O'Boyle, H. Hamann, and S. McNab, Nature **438**, 65 (2005).
- [14] M. Kaniber *et al.*, Phys. Rev. B **77**, 073312 (2008).
- [15] E. Viasnoff-Schwoob *et al.*, Phys. Rev. Lett. **95**, 183901 (2005).
- [16] A. F. Koenderink, M. Kafesaki, C. M. Soukoulis, and V. Sandoghdar, J. Opt. Soc. Am. B **23**, 1196 (2006).
- [17] J. M. Smith *et al.*, Phys. Rev. Lett. **94**, 197402 (2005).
- [18] J. Johansen *et al.*, Phys. Rev. B **77**, 073303 (2008).
- [19] S. G. Johnson and J. D. Joannopoulos, Opt. Express **8**, 173 (2001).
- [20] S. Hughes, L. Ramunno, J. F. Young and J. E. Sipe, Phys. Rev. Lett. **94**, 033903 (2005).
- [21] W.-H. Chang *et al.*, Phys. Rev. Lett. **96**, 117401 (2006).